Hydration forces at solid and fluid biointerfaces

Buddha R. Shrestha, Xavier Banquy

Canada Research Chair in Bio-Inspired Materials and Interfaces, Faculty of Pharmacy, Université de Montréal, PO Box 6128, Montréal, QC H3C 3J7, Canada

* Corresponding author: xavier.banquy@umontreal.ca

Abstract

We review the different molecular mechanisms giving rise to the repulsive hydration force between biologically relevant surfaces such as lipid bilayers and bio-ceramics. As we will show, the hydration force manifests itself in very different and subtle ways depending on the substrates. Soft, mobile surfaces such as lipid bilayers tend to exhibit monotonic, decaying hydration force, originated from the entropic constriction of the lipid head groups. Solid surfaces on the other hand, tend to exhibit a periodic oscillatory hydration force, originated from the surface induced polarization of water molecules. In this review we will describe both subtle faces of this important interaction by first describing the early experiments performed on solid surfaces and their interpretation by recent simulation studies. Then we will describe the hydration force between fluid interfaces such as bilayers and explain how experimentally researchers have unraveled the dominant role of the lipid head groups conformation.

INTRODUCTION

For decades, it was perceived that the Derjaguin Landau Verwey and Overbeek (DLVO) theory[1, 2], a combination of repulsive electrical double layer forces and attractive van der Waals forces, is able to describe the properties of wide range of colloids and bio-colloids. According to this theory, at separations below 2-4 nm, attractive van der Waals forces always dominates over the repulsive double layer forces leading to an adhesive contact. However, several phenomena (re-peptization, hydrophobic colloids, and silica particles) were found not to obey this theory as these materials neither coagulated nor swelled as predicted by DLVO theory. Thus, the idea of a repulsive force, the hydration force, acting at a few nanometer separation distance, overcoming the van der Waals primary adhesive minimum arose. These observations, yet, were not sufficient to prove the existence of an additional force simply because other repulsive contributions such as the Stern layers compression or the possible presence of steric repulsive interactions had to be ruled out [3]. Frens and Overbeek [4, 5] proposed a model which explained the removal of the primary adhesive minimum by shifting the hard wall cut off to a finite separation of $D = D_0 + 2d$, where D_0 was the zero distance and d the diameter of ions. This theory showed that the net repulsion could continue to rise steeply as the inter-particle distance separation decreased to contact even when the surface charge density or potential was low. After this first intent, the necessity of directly measuring the interaction forces vs. separation distance was the subject of intense research in order to experimentally verify if the force laws measured can be fitted using DLVO-Stern model or if it requires some extra force to be fitted. In what

40 follows, we will describe the experimental characterization of the hydration forces, in two main
41 systems, namely lipid membranes and solid substrates, the apparent discrepancies in the
42 experimental observations that have emerged and the common ground between different
43 researches. We describe the various experimental methods that are still used to determine such
44 forces and continue with a detailed description of the results obtained from Surface Force
45 Apparatus (SFA).

46 **FORCE MONITORING TECHNIQUES**

47 Several direct force measuring techniques have been developed till date. Some were
48 devised for specific purposes while others have been implemented for a broad range of
49 applications. The first technique to provide the quantitative data into the short range hydration
50 forces is the Osmotic Pressure (OP) technique. OP is able to measure the repulsive forces in
51 aqueous solutions between surfactants or lipid bilayers [6-8], aligned clay sheets [9, 10] and
52 aligned macromolecules [11]. In this method, osmotic pressure is applied to the aqueous sample
53 and the equilibrium spacing between surfaces is monitored by X-rays. This technique, however,
54 is unable to measure interaction forces at longer range and is thus limited to only the repulsive
55 parts of the force laws. OP is not able to detect any adhesive forces. Later, SFA was developed
56 by Tabor, Winterton and Israelachvili [12-14] to measure the van der Waals forces between
57 molecularly smooth mica surfaces in air or vacuum. Israelachvili further modified the apparatus
58 and enabled it to monitor forces in liquid medium as well. This opened the gateway to the broad
59 field of modern surface science for instance rheology [15], tribology [16], sensing [17],
60 electrochemistry [18], corrosion [19].

61 Figure 1A shows the schematic representation of the SFA apparatus. A white light beam
62 is directed through two curved discs covered with back-silvered mica sheets of thickness 2 to 5
63 μm. The silver thickness on mica is about 45 nm to 50 nm to allow at least 95% reflection. The
64 discs are placed in cross cylinder geometry creating a three layer interferometer. The interference
65 fringes emerging from the apparatus are called fringes of equal chromatic order (FECO). The
66 transmitted light is directed to a spectrometer for further analysis of FECO fringes. The
67 interaction force, F, acting between the surfaces is measured by the deflection of a spring on
68 which one of the surfaces is mounted [20]. This technique has distance and force resolutions of 1
69 Å and 1 μN respectively [21]. The detailed description of the instrument is given in ref. [22].
70 Using white light interferometry, the separation distance, the radius of curvature and the
71 interacting force can be in-situ monitored in SFA experiments.[23] Hence, absolute distance
72 referencing and normalization of the measured forces by radius of curvature remain
73 unambiguous. Yet, in SFA experiments, the contact area is macroscopic and typically in the
74 range of hundreds or thousands of μm^2 which is much larger than that the typical contact area
75 measured in single molecule force spectroscopy [24].

76 The Atomic Force Microscope (AFM) technique is widely used to measure interaction
77 forces between surfaces at the molecular scale[24]. The schematic of AFM is shown in Figure
78 1B. In an AFM experiment, a small tip attached to a lever is moved toward a surface. Meanwhile
79 the deflection of the lever and the displacement of the base to which the lever is mounted are
80 measured as shown in Figure 1B. The deflection of the lever is measured using a laser beam
81 reflected into a four quadrant diode and converted into interaction force using Hooke's law. The
82 zero distance (the situation at which the tip is in contact with the sample) in an AFM experiment,
83 however, is assumed by calibration with a hard wall of unknown origin. The exact shape and the

84 roughness of an AFM tip in contact with the surface is usually unknown which often complicates
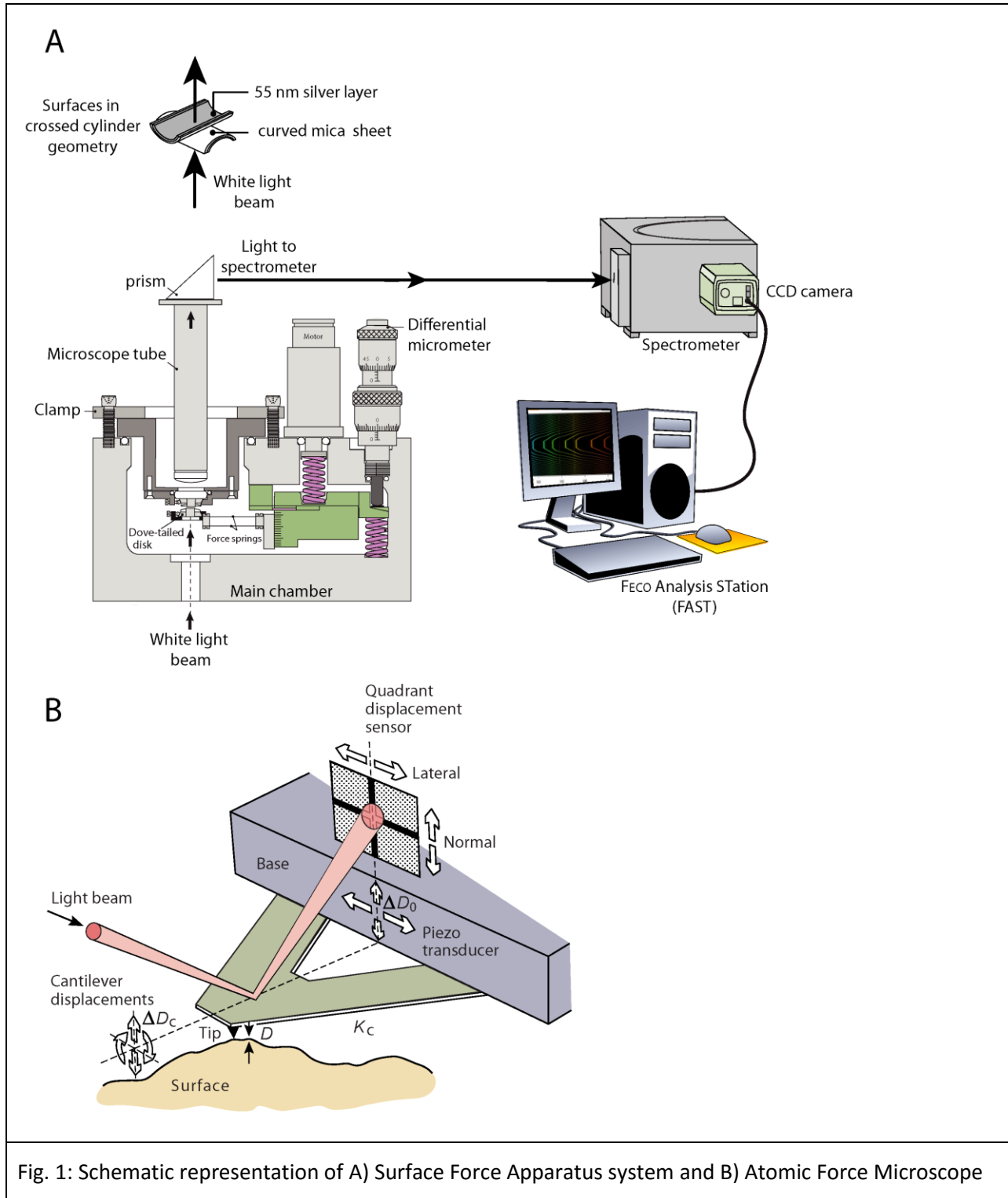85 the direct comparison even between different AFM experiments.

Fig. 1: Schematic representation of A) Surface Force Apparatus system and B) Atomic Force Microscope

86

87   In this report, we review the origin and evolution of the repulsive hydration force in
88 various electrolyte solutions taking into account especially the SFA results, and corroborate the
89 results by simulation and other experimental techniques wherever applicable.

90 **FORCES BETWEEN SOLID SURFACES IN ELECTROLYTE SOLUTION**

91   The very first, accurate and direct measurement of forces between solid mica surfaces
92 immersed in aqueous electrolyte using SFA by Israelachvili and Adams [25] is shown in Figure
93 2 (the results obtained by Pashley el al. is also combined in Figure 2A). It shows the forces
94 between two charged hydrophilic mica surfaces in K^+ solutions in the concentration range of 1 to
95 10^{-5} M at 20^0C at pH 6. Figure 2A shows pure DLVO interaction below 10^{-3} M and an additional
96 monotonic short range repulsion at or above this concentration for K^+ ions. Pashley boldly
97 reported the rise of hydration forces only above *a certain critical bulk concentration which*
98 *depends on the electrolyte* [26]. Hydration forces become apparent only when hydrated cations
99 adsorbed on mica are prevented from desorbing the surfaces upon approach. Pashley showed that
100 this force *is completely absent at* $\sim 5 \times 10^{-6}$ *M for* Na^+ *and in hydrochloric acid solutions up to*
101 *1.2* $\times$ *10^{-3} M* [27]. Pashley and Israelachvili [28] further reconfirmed the rise of an additional
102 short-range repulsive hydration force only above a certain electrolyte concentration by careful
103 examination of the interaction forces below 2 nm of separation distance in aqueous KC1
104 solutions. The authors showed that the increase of the hydration force occurred both in
105 magnitude and range (attaining 4–5 nm) with the increase of adsorbed ions on the surface.
106 Pashley calculated the magnitude of the hydration force which followed the series $Na^+ > Li^+ >$
107 $K^+ > Cs^+$ using a simple site-binding model to describe the charging behavior of interacting mica
108 surface [29]. The DLVO-regulation theory was subtracted from the total measured force on the
109 assumption that the mica surfaces apparently were fully covered with adsorbed cations.
110 Qualitatively, with the exception of sodium, it seemed that the smaller the ions the stronger is its
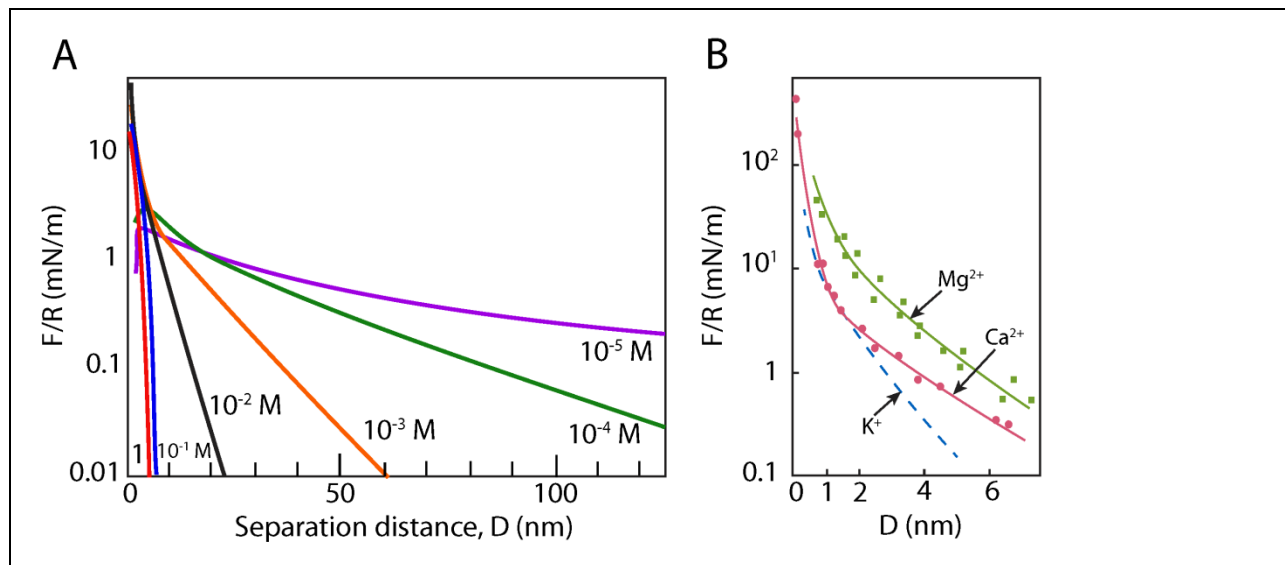

Fig. 2 A: Semi-logarithmic plot of force vs. distance measured between curved mica surfaces in aqueous
K^+ solution ranging from 10^{-5} M to 1 M. B: Comparison of the hydration force of monovalent K^+ of 10^{-1} M
with divalent ions Mg^{2+} and Ca^{2+} of 3 M and 5 M respectively . Adapted from ref [25-29] and [32].

111   binding capacity to mica. Similar results were observed by Hribar *et al.* and Goldberg *et*
112   *al.* [30, 31].

113   Pashley and Israelachvili [32] also measured the interaction forces between mica surfaces
114   in divalent metal (Mg^{2+}, Ca^{2+}, Sr^{2+}, and Ba^{2+}) chloride solutions. They found that at
115   concentrations $\geq$ 1.0 M, the divalent cations firmly bind to the interacting mica surfaces giving
116   rise to a repulsive short-range force (see Figure 2B) seemingly due to the residual hydration
117   shells of the bound cations. The authors inferred that the divalent cations were more strongly
118   hydrated than monovalent cations and therefore did not easily shed their hydration layers in order
119   to bind to the mica surface and give rise to hydration force at higher concentrations than
120   monovalent cations do. The magnitude of the hydration force followed the series $Mg^{2+} > Ca^{2+} >$
121     $Li^+ \sim Na^+ > K^+ > Cs^+$. Israelachvili and Adams also observed that the double layer forces were
122   much reduced in $Ca(NO_3)_2$ and $BaCl_2$ solutions compared to those in KNO_3 solutions and were
123   not accurately described by DLVO theory [33]. Using a modified set up of SFA, Rabinovich *et*
124   *al.*[34] carried out direct measurements of the interaction forces between gold spheres and
125   crossed quartz filaments in air within the region of distances from 10 to 100 nm. The authors
126   observed deviations from DLVO theory below 5 nm which they attributed to the influence of
127   structural forces. Ruckenstein *et al.* [35] suggested that bilayers of charges formed by the
128   adsorption of hydrated ions and that charged bilayer generated a polarization in the neighboring
129   water molecules which propagates into the liquid. The repulsive hydration forces were generated
130   by the overlap of the polarization layers of the two plates.

131   All the mentioned studies confirmed independently the existence of an interaction force,
132   different from the normal van der Waals and double-layer forces. This force was found to be
133   independent to the type of electrolyte. Therefore it was classified as an additional force and not a
134   modification of the double-layer force. Hence, for the first time, the repulsive forces which later
135   will be defined as hydration forces was introduced. The general inference that is drawn by these
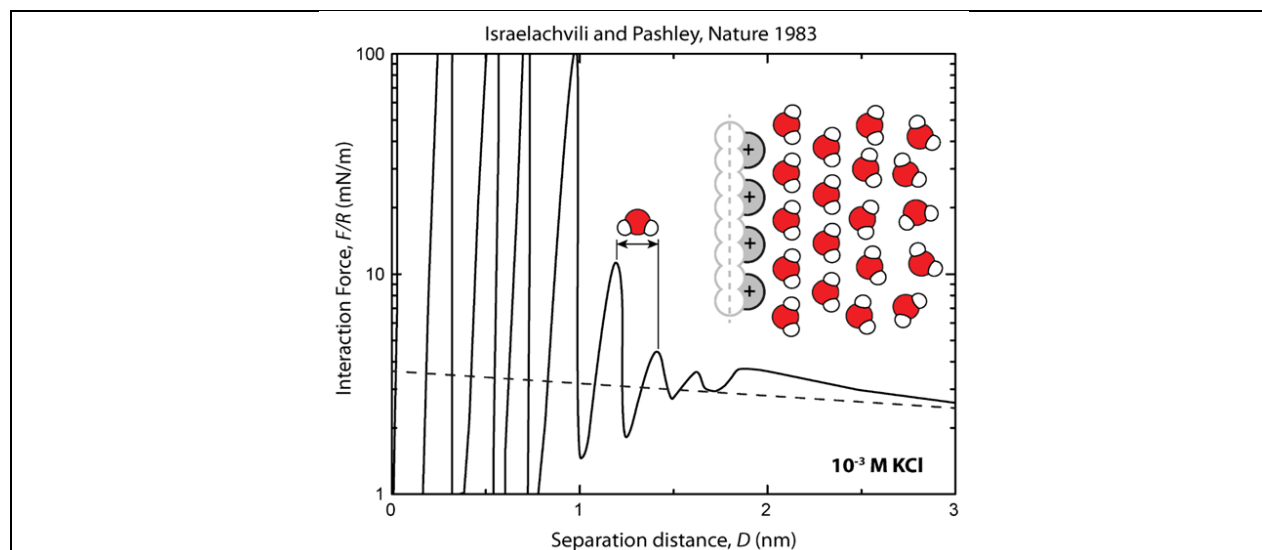136   *early* studies is that the force was intrinsically repulsive and decayed *monotonically* with

Fig. 3 Force measured between two curved mica surfaces as a function of distance in 10^{-3} M KCl solution. Adapted from ref [38].

137 distance out to a separation distance of around 5 nm.

138 On one hand, these results were considered as a breakthrough since the full force law
139 was possible to be determined/verified experimentally but on the other hand, they were
140 contradicting the results of computer simulations [36, 37] which were predicting an oscillatory
141 density profile extending several molecular diameters into the liquid. Abraham [36] suspected
142 that the hydration force would probably arise between hydrophilic surfaces, such as silica and
143 mica, since strongly H-bonding surface groups modify the H-bonding network of nearby liquid
144 water molecules.

145 In 1983 Israelachvili and Pashley[38] meticulously measured the hydration force in 10^{-3}
146 M KCl solution of pH 5.5 between molecularly smooth mica surfaces. The authors reported that
147 the hydration force was not monotonic once the separation distance was smaller or equal to 20 Å.
148 The hydration force was oscillatory having a minima and maxima of periodicity 2.5 ± 0.3 Å,
149 roughly the diameter of a water molecule (Fig. 3). The schematic in Figure 3 shows that the
150 adsorption of ions on the mica surface orders water molecule at the surface. Using atomic force
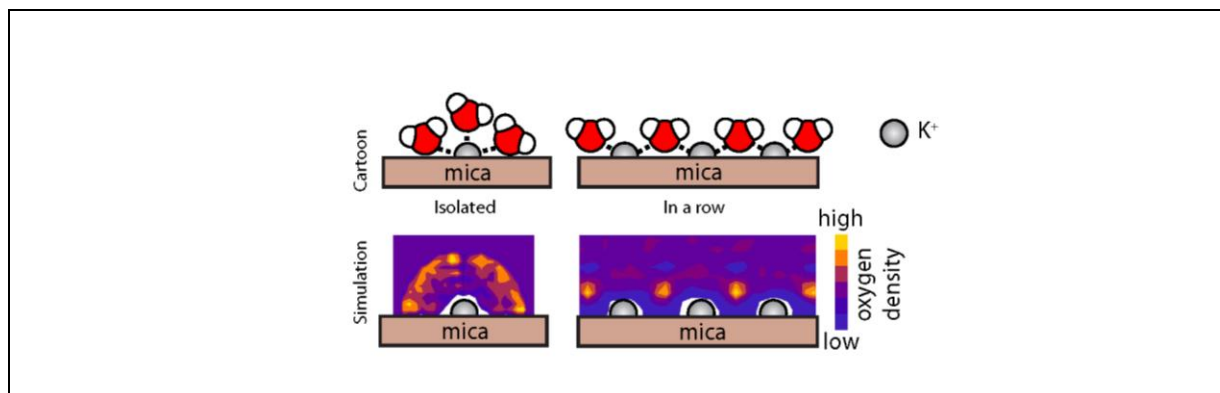151 microscopy(AFM) and computer simulations, Ricci *et al.* [39] recently showed that cations

Fig. 4: The schematic representation of cation/s (K$^+$) being randomly adsorbed (a) and adsorbed
forming a row on mica (b). Similarly c and d represents the density of oxygen atoms of the water
molecules. In the case of single ion, the value of oxygen density is the radial average around K$^+$ ions.
In the latter case, the average oxygen density is obtained by considering a rectangle of 0.5nm width
aligned with the row of the ions and centered on them. Adapted from ref [39].

152 adsorbed on the surface of mica could induce ordered water layers at the surface of
153 homogeneous solids in aqueous solutions as shown in Figure 4. Similar results were reported in a
154 recent study using molecular dynamics simulations between two mica surfaces in an aqueous
155 KCl electrolyte solution by Leng *et al.* [40]. Urbic *et al.* [41] also came to the same conclusion in
156 a simulation study. The authors used the Mercedes-Benz (MB) model of water, in NVT and µVT
157 Monte Carlo computer simulations and observed oscillations in the forces between inert plates,
158 due to water structure, even at plates separation of 5-10 water diameters. Cherepanov *et al.* [42]
159 showed the increase of the hydration repulsion with ionic strength by molecular dynamics
160 simulation. Henderson *et al.* [43] reported 7 force oscillations below 2 nm between spheres
161 brought in contact using a non-continuum molecular theory. Using grand canonical molecular-
162 dynamics simulations. Li *et al.* [44] reported oscillatory solvation forces between hydrophilic
163 mica and glass surfaces. Fenter *et al.* [45, 46] studied the mica (001)-water interface under
164 ambient conditions using High-resolution x-ray reflectivity. The results revealed density

oscillations of the water oxygen atoms in the normal direction to the surface, providing evidence of interfacial water ordering. The spacing between neighboring water layers in the near-surface region, were approximately 2.5(2) – 2.7(2) Å, close to the size of a water molecule. The density oscillations extended to about 10 Å above the surface and did not strictly maintain a constant periodicity. The authors came to the conclusion that the primary hydration layer was followed by a weakly modulated hydration structure that extended more than 1 nm above the surface.

The described experimental and simulation results show that for monovalent ions the hydration force between hard surfaces appears only above a critical ion concentration and is not only monotonically repulsive but has an oscillatory component superimposed to it.

Attempts have been made to measure the forces between surfaces other than mica. Horn *et al.* [47] measured the monotonic short-range repulsive force devoid of oscillatory component in NaCl solutions between silica surfaces. The measured force was found insensitive to the ionic conditions making it apparently intrinsic to the surfaces. Similar forces have been measured between silica surfaces by Vigil *et al.* [48], Ducker *et al.*[49], between mica surfaces by Shubin *et al.* [50], between (0001) sapphire surfaces by Drucker *et al.* [51], and between glass fibers by Rabinovich *et al.*[34] using different techniques. According to Iler [52, 53], silica is amorphous and its negative surface charges are located at the ends of short silica hairs protruding a few angstroms from the surfaces which shifts the Outer Helmholtz Plane farther out than the physical solid-liquid interface (the van der Waals plane) causing the DLVO interaction to be more repulsive. A similar effect is observed for finite sized counterions adsorbed on mica surfaces [54, 55]. Chapel [56] measured forces between two pyrogenic silica sheets immersed in monovalent electrolytes (CsCl, KC1, NaC1, LiC1). Contrary to the previous results, his results showed that the strength and the range of the hydration force decrease with increasing the degree of hydration of the counter ion. This is opposite to the behavior of mica for which adsorbed counter ions have been reported to generate a hydration repulsion. The effects of counter ions on hydration forces, weakening for silica and enhancing for mica, show that the origin of the short-range interaction is not unique.

The existence of hydration force was evidenced by several researchers using various modes of AFM [49, 57-67]. As postulated by Israelachvili *et al.*[21], experimentally shown by Atkins *et al.* and Zeng *et al.*[68, 69], and theoretically shown by Yang *et al.* [70]; a tip roughness greater than the molecular diameter of the water molecule plays an important role in smearing out the oscillatory component of the hydration force. Adsorbed chemical compounds can also alter significantly the stability of the hydration layer as recently shown by Akrami *et al.* [71]. Direct *in situ* characterization of the AFM tip or of any interacting surface cannot be performed till date which limits our understanding of the role of surface roughness or chemistry in the appearance or disappearance of hydration forces. For more details, readers are suggested to consider refs [68, 72-77].

As discussed, the simulation studies have always been leading showing the layered density profile [36, 78-80] analogous to the hydration shell and/or evidences of interfacial layering near interfaces [81-93] for various types of substrates. Layered density profile were also experimentally shown under potential control [94-97]. The recent advancement of X-ray techniques [98-103] have enabled atomic-scale studies of interfaces. Liquid density oscillations near solid surfaces have been observed in many systems [104-108]. Neutron scattering

208 measurements have also demonstrated the existence of structured fluid layers under confinement
209 [88, 89], [109-112]. Mineral-water interface using X ray has been studied by Fenter et al. [46,
210 113-118]. For details mineral–water interfacial structures revealed by synchrotron X-ray
211 scattering refer to references [45, 119]

212   Thus from above close examination of the studies, both experimental and theoretical, we
213 can draw the following conclusions:

214 1. Above the critical concentration, the adsorption of cation on the mica surface is the cause
215   of the repulsive hydration force and the hydration force is not only monotonically
216   repulsive but an additional oscillatory component is superimposed to it below 2 nm and
217   its periodicity is equal to the mean molecular diameter of water.
218 2. The critical concentration depends on the type of the electrolyte. The critical
219   concentration for divalent metal ion is always higher than that for the monovalent metal
220   ion solution.
221 3. The magnitude of the oscillatory force component depends on the extent of adsorption of
222   cation on the surface which in turn depends on the concentration of the solution. The
223   more the cations adsorbed the strong is the hydration force.
224 4. Surface roughness plays an important role in smearing out the oscillatory component of
225   the hydration forces.

226
227

HYDRATION FORCES BETWEEN LIPID BILAYERS

228

229 Lipid bilayers have been extensively studied in the past 50 years. Lipid bilayer are formed by
230 the self assembly, in water, of lipid molecules into a bilayer structure through hydrophobic
231 interactions between hydrocarbon tails of the molecules. As a consequence, the interfacial
232 properties of a bilayer differs significantly from those of solid surfaces mostly due to the inherent
233 mobility of the lipid molecules forming the bilayers. As we will see, such mobility dramatically
234 modulates the interaction of the bilayer with water molecules, solvated ions and with other
235 bilayers as well. In what follows, we describe the recent efforts that have been made towards a
236 better understanding of such interactions and the future directions of research that these recent
237 results are offering.

238 *The water-bilayer interface*

239 The structure of the water bilayer interface has been studied extensively using spectroscopic
240 techniques such as Nuclear Magnetic Resonance (NMR) and Infrared (IR spectroscopy).[120]
241 Early studies performed using NMR and molecular dynamic simulation (MDS) focused on
242 identifying the number of molecules necessary to form the hydration shell of lipids. It is
243 commonly accepted that this number varies between 17-22 water molecules depending on the
244 lipid head group, lipid area [121] and availability of ions or solutes and temperature (see Figure
245 5).[122] More recent simulations have suggested that the interfacial water can mostly be
246 classified into three categories which are [123, 124] (i) buried water located close to the
247 carbonyl groups, (ii) first external hydration shell near the phosphorylcholine groups and (iii)
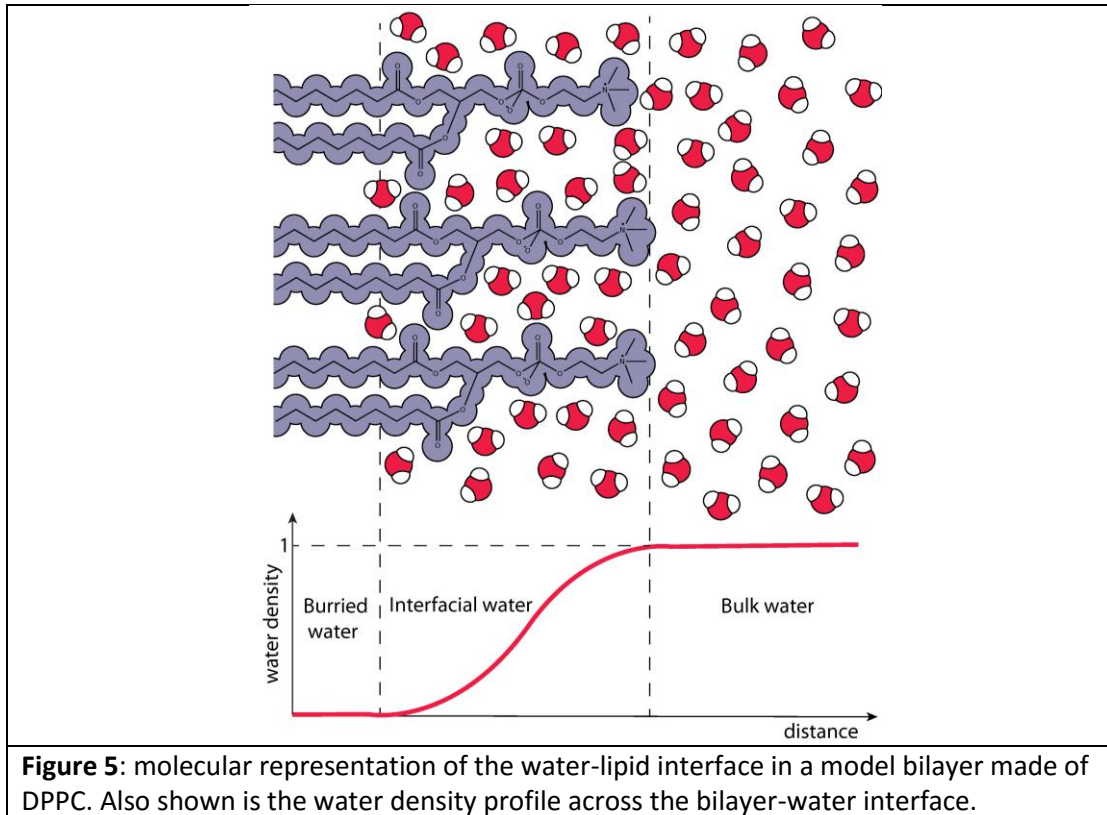

Figure 5: molecular representation of the water-lipid interface in a model bilayer made of DPPC. Also shown is the water density profile across the bilayer-water interface.

248 secondary hydration shell. Even though such classification has not been confirmed

249 experimentally, there are clear experimental evidences of strongly bound water molecules to
250 lipid head groups.

251   Water distribution around lipid head group can be easily disturbed by external factor. In
252 particular, presence of ions, especially cations have been shown experimentally to alter lipid
253 molecular area and diffusivity. Since Na^+ is the most physiologically abundant, its interaction
254 with lipid bilayers has been extensively studied, theoretically and experimentally. For example
255 Fluorescence Correlation Spectroscopy (FCS) has been used to characterize POPC self-diffusion
256 coefficient in presence of varying concentration of NaCl at different temperatures. The study
257 shows that independent to the fluorescent marker used, the augment in concentration of salt tend
258 to decrease the diffusion of POPC molecules.[125] Simulation studies confirmed this observation
259 and revealed that tight coordination complexes involving one Na^+, three lipid molecules and 1-2
260 water molecules could be formed. Similar results were reported with mixed lipid bilayers.[126]

261 The binding of other types of species such as organic molecules have also been reported to
262 strongly affect the behavior of water molecules near the bilayer interface. For example, dimethyl
263 sulfoxide (DMSO) has been widely studied for its ability to preserve cellular membrane during
264 cryo-preservation. Such important property was recently explained using PFG NMR and the
265 SFA.[127]

266 *Interaction forces between lipid bilayers*

267 The interaction forces acting between apposing lipid bilayers include the following: [52]

268   (i)   van der Waals interactions forces between the bilayer hydrocarbons layer across
269   water,
270   (ii)   hydration forces due to the expulsion of water molecules upon compression of the
271   bilayers,
272   (iii)   the hydrophobic interaction between lipid tails across water,
273   (iv)   the protrusion interaction forces due to the restriction of lipids position
274   fluctuations along the direction of compression,
275   (v)   the lipid head group overlap involving conformational change of the head groups
276   upon compression,
277   (vi)   the undulation forces due to bending fluctuations of the bilayers and
278   (vii) the electrostatic interaction forces due to bilayer surface charging.

279 Each of these contributions have been studied both experimentally and theoretically.
280 Mathematical expressions of these interactions are provided in Table 1 and the reader is referred
281 to the original references for further details of their derivation.

282 Interaction forces between lipid bilayers or lipid membranes have been measured using a variety
283 of techniques. The two main techniques have been the osmotic pressure technique (OP) and the
284 SFA. As can be seen in Figure 6A and B, both measurement techniques give similar results on
285 single component lipid bilayers and multi-component lipid bilayers/membranes. Important
286 differences should also be noticed: when using the OP technique, the thickness of the lipid
287 bilayers increases (the lipid molecular area decreases) as the applied pressure increases; while in

288   the SFA measurement, the lipid bilayer becomes thinner (the molecular area increases) at the
289   contact area due to lateral diffusion of lipids during the compression. These important
290   differences explain why hemifusion/fusion of bilayers is rarely reported using the OP technique
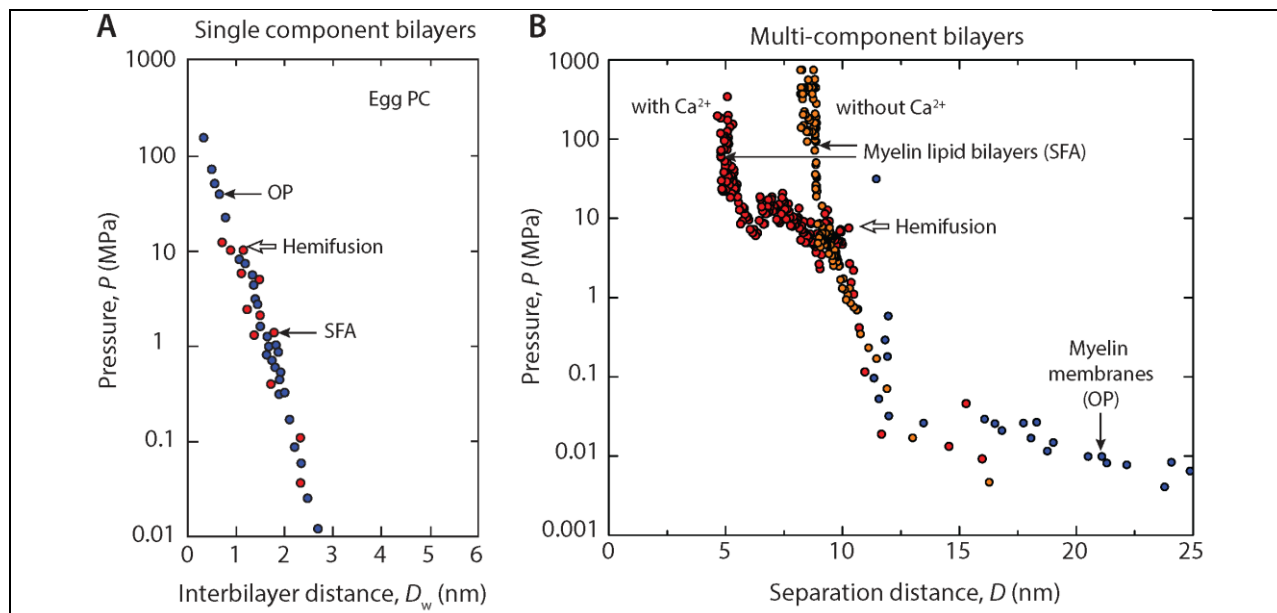291   and can be easily observed using the SFA.

Figure 6: Short range forces measured between single component lipid bilayers (A) and multi-component lipid bilayers and lipid membranes (B). **(A)** Interaction forces between lipid bilayers of egg PC measured independently with the SFA and by the osmotic pressure technique (OP). Both measurements show the presence of a net repulsive force exponentially decreasing with the bilayer separation distance. The characteristic decay length of this interaction is 2.5 Å. Note that in the SFA experiment only, membrane hemifusion is observed at a pressure of 10 MPa [128] **(B)** Interaction forces between multi-component membranes. Measurement performed between myelin lipid bilayers using the SFA in buffer saline show that addition of calcium in the medium promotes hemifusion of the membranes. Experiment performed with the osmotic pressure method show the interaction forces between integral myelin membranes from [129]. The results illustrate that the long range portion of the interaction forces measured by SFA and OP, mainly caused by the electrostatic interaction, are in very good agreement besides the presence of transmembrane proteins in the myelin membranes which are absent in myelin lipid bilayers. Interestingly, myelin membranes do not present any signs of hemifusion during the experiment while hemifusion was clearly observed with the SFA at a surface pressure of approximately 7-10 MPa. Adapted from Refs [129], [130], [139]

292

Table 1: Interaction forces commonly encountered at lipid bilayers and at solid surfaces

Contribution	Equation		Reference
Head group overlap	$P(D) = \frac{kT}{s^3}\left[\left(\frac{2L}{D}\right)^{9/4} - \left(\frac{D}{2L}\right)^{3/4}\right]$ for $D < 2L$	(Eq. 1)	[130, 131]
	$P(D) = \frac{100}{s^3}kTe^{-\pi D/L}$ for $0.4L < D < 1.8L$	(Eq. 2)	
Undulation	$P(D) = \frac{3\pi^2 (kT)^2}{64 k_b D^3}$	(Eq. 3)	[132]
Hydrophobic interaction	$P(D) = -\frac{e^{-D/D_H}}{D_H}\left[\left(1 - \left(1 - e^{-D/D_H}\right)^{1/2}\right) + \frac{1}{2}\left(e^{-D/D_H}\left(1 - e^{-D/D_H}\right)^{-1/2}\right)\right]$	(Eq. 4)	[133-135]
Protrusion interaction	$P(D) = 2.7(\Gamma kT/\lambda)e^{-D/\lambda}$ $\lambda = kT/\pi\delta\gamma_i$	(Eq. 5)	[136, 137]
van der Waals	$P(D) = \frac{-A}{6\pi D^3}$	(Eq. 6)	[52]
Electrostatic	$P(D) = 64kT\rho_\infty \tanh^2(ze\psi_0/4kT)e^{-D/\lambda_D}$	(Eq. 7)	[52]
Hydration	$P(D) = W_0 e^{-D/D_H}$	(Eq. 8)	[52]
Oscillatory (structural)	$P(D) \approx W_0/\sigma \, e^{-D/\sigma}\left[2\pi \sin\frac{2\pi D}{\sigma} - 1\right]$	(Eq. 9)	[52]

It is important to note that all these interaction forces originates from very distinct causes and therefore exhibit very different magnitudes and act over very different length scales. As a consequence, the separation distance D between the bilayer does not have the same origin point or (operational plane) in each contribution.[52] For example, the plane of origin of the electrostatic interaction should be located at the position where surface charges are located which might be quite different from the origin plane of the van der Waals interaction. Shifting of the plane of origin of an interaction potential is usually done by replacing the separation distance D by $D-D_0$ where D_0 is the shifting distance.

All the interactions presented in Table 1 do not have to be necessarily considered in every situation. For example in a physiological fluid or in a buffer saline solution containing salt concentrations of typically 150 mM (1:1 electrolyte), the van der Waals interaction is usually found to be negligible compared to other contributions. The presence of free ions in the medium

307 screens the zero-frequency term of the van der Waals interaction over a distance equals to the
308 Debye screening length (roughly 1 nm at physiological conditions).

309 The hydrophobic interaction is usually considered to play a minor role in the total interaction
310 between bilayers mainly because it is generally counterbalanced by other contributions such as
311 the electrostatic or the head group overlap force. Hydrophobic forces should only be considered
312 when hemifusion/fusion of the bilayers occurs. As the bilayers are compressed, thinning will
313 start to occur and will favor the exposure of the hidden hydrophobic core of the bilayer to the
314 aqueous medium. It is clear then that appearance of the hydrophobic interaction between facing
315 bilayers depends on lipids molecular coverage and its variation with confinement. Donaldson *et*
316 *al.* [133] provided a simple expression for the molecular area of *elastic* lipid bilayers in presence
317 of the hydrophobic interaction:

$$318 \qquad a(D) = a_0\big(1 - e^{-D/D_H}\big)^{-1/2} \qquad\qquad\qquad \text{(Eq. 8)}$$

319 Using the expression of the hydrophobic interaction together with the electrostatic and steric
320 contributions, Banquy *et al.* described the interaction forces between two model myelin lipid
321 bilayers immersed in buffered saline solution.[138] The authors showed that consideration of the
322 hydrophobic interaction allowed to predict the onset of hemifusion of the bilayers which
323 occurred when the lipid molecular area increased by almost 30% (see Figure 7A). The critical
324 molecular area at which hemifusion appears, i.e. the point where the hydrophobic interaction
325 counterbalances all other repulsive interactions, is strongly dependent on the cohesive strength of
326 the bilayers and the lipid molecular area.

327 Figure 7B presents a situation where a photosensitive bilayer was deposited on mica by the
328 vesicle deposition method. When compressed, the bilayers hemifused at a critical molecular area
329 which was 16% higher than the equilibrium value. When illuminated under UV light, the
330 surfactant molecules changed conformation and became more hydrophilic which dramatically
331 expanded both the interfacial energy and the molecular area of the molecules at rest. Thus, the
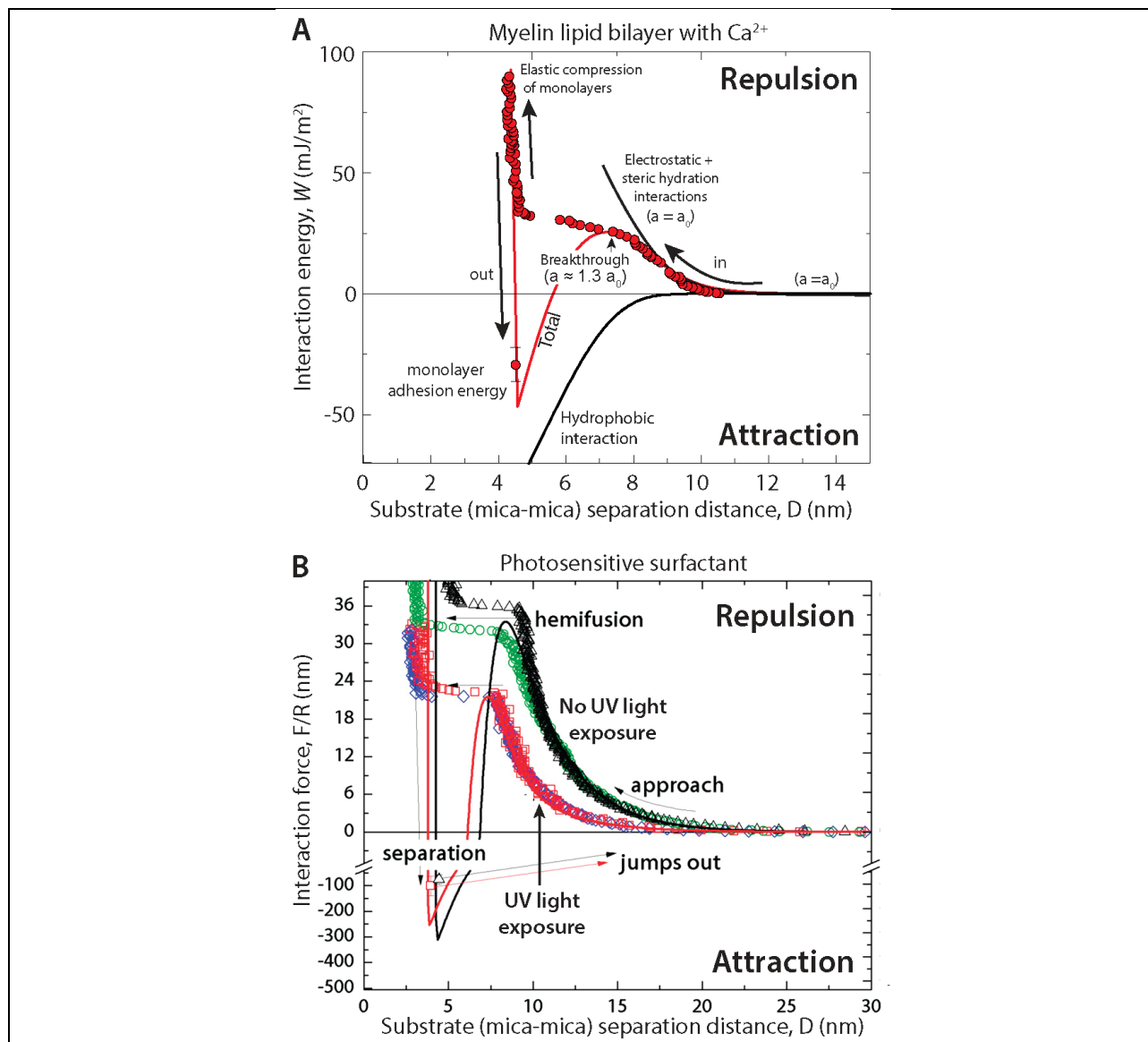332 critical molecular area at hemifusion was found to be 25% higher than the value at equilibrium.

Figure 7: (A) Interaction energy between two myelin lipid bilayers in presence of 2 mM Ca²⁺ ions. Calcium ions facilitate the hemifusion of the bilayers as denoted by a breakthrough instability in the interaction energy profile. Such instability is governed by the hydrophobic interaction between the hydrocarbon tails of the lipids that are being exposed during compression and thinning of the bilayers. Adapted from [139] (B) Interaction force measured between photosensitive surfactant bilayers. In this system the hydrophobic force was modulated by the exposure of the light sensitive hydrocarbon tails to UV light leading to different energetic barrier to hemifusion. Adapted from [139]

333

The undulation interaction has by far the longest range and is comparable in magnitude to the van der Waals interaction. The magnitude of this interaction can be strongly by different external parameters. For example, lipid bilayer supported on a solid substrate will almost no undulations. As shown in Eq. 3, undulation forces are also extremely sensitive to temperature which can be useful in experimental settings where fine tuning of this interaction is required. Ions have also an important impact on undulation forces. Free ions in solution can either adsorb on lipid

14

membranes, alter head group dissociation degree or their hydration level. All these factors will impact directly or indirectly the bending modulus of the bilayer and therefore the undulation forces. For low salt concentration (or large surface charges),[140] derived the following expression for the bending modulus of symmetrical bilayers:

$$k_b = \frac{\varepsilon \lambda_D}{\pi}\left(\frac{kT}{e}\right)^2 \qquad \text{(Eq. 9)}$$

Considering that $\lambda_D = 0.304/\sqrt{C}$ for a 1:1 electrolyte at room temperature, simplification of Eq. 9 leads to $P \propto \sqrt{C}$ which results in a weak dependence on salt concentration. In the high salt regime, the expression of the bending modulus becomes:

$$k_b = \frac{3\pi(\lambda_D)^3\sigma^2}{\varepsilon} \qquad \text{(Eq. 10)}$$

where σ is the surface charge and ε the dielectric constant of the medium. Using the Grahame equation for a 1:1 electrolyte, the expression for σ becomes $\sigma = \sqrt{8\varepsilon\varepsilon_0 kT}\sinh(e\psi_0/kT)\sqrt{C}$ which leads to the same weak dependence for the interaction pressure $P \propto \sqrt{C}$.

The head group overlap and protrusion forces are usually difficult to distinguish from each other and are often termed "steric hydration" forces. The protrusion force is related to the hydrophilicity of the bilayer while the head group overlap force is more related to the hydration of the head groups. In both cases, it is important to remember that these forces do not originate from water structuring at the bilayer-water interface. Since both interactions exhibit an exponential decay (see Eq. 2 and 5), comparison of their characteristic decay length should in principles provide useful insights into the contribution that dominates the total interaction. A back of the envelope calculation already provides good estimates of the expected values of these two parameters. Considering the interfacial tension between water and hydrocarbon to be 50 mJ/m^2 and the cross sectional radius of the hydrocarbon chain to be close to 0.2 nm, we found using Eq. 5, $\lambda = 0.13$ nm. On the other hand, the size of a phosphatidyl head group is expected to be close to 0.8 nm giving (Eq. 2) $\lambda = 0.25$ nm. Since these two decay lengths are comparable, it is a priori difficult to identify the dominant one.

In a recent study by Schrader *et al.* [141], the authors characterized the effect of DMSO, in water, on the interactions between bilayers. The authors elegantly demonstrated that by increasing the concentration of DMSO in water from 0% to 7.5%, the decay length of the interaction force markedly decreased from 0.2 to 0.15 nm (see Fig. 9). Since the interfacial tension between water/DMSO and hydrocarbon decreases with increasing the DMSO content, it is clear that the measured change in decay length could not be accounted by the presence of protruding forces. However, using NMR diffusion measurements, the authors showed that the change in decay length observed in presence of higher concentrations of DMSO was correlated with a change in hydrodynamic radius of the head group ionic moieties. The authors concluded that the interaction forces between DPPC bilayers at separation distance lower than 2 nm were dominated by the head group overlap force which is tuned by the competition between DMSO and water molecules to interact with the lipid head group.
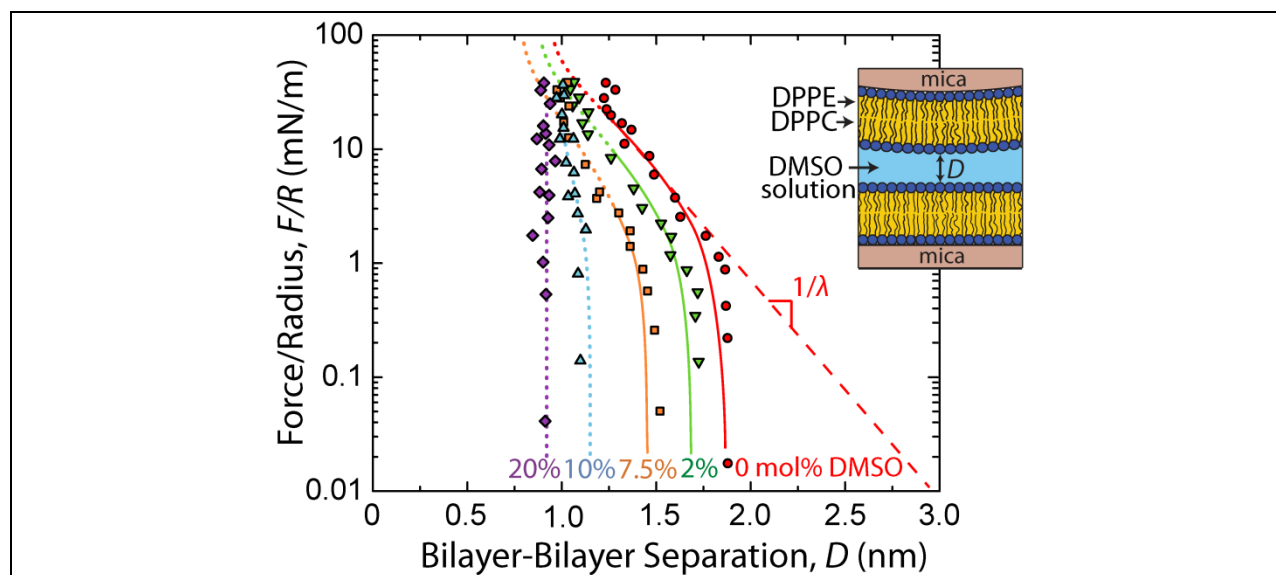
15

377

Fig.8 Short range interaction forces measured between DPPC lipid layers in presence of a water-DMSO solution. Measurements show a decrease of the range and the decay of the interaction forces which is a characteristic signature of a conformational change of the lipid head group mediated by DMSO. Adapted from [142].

These recent and previous studies [142-144] underscore the important fact that the so called "steric hydration" is actually an steric-entropic force similar to the polymer-brush interaction described by Alexander and deGennes. The role of water is solely to modulate the hydration, and therefore the conformation, of the lipid head groups. The effect of water on the degree of hydration of a lipid head group is a solvation effect which in term of interaction forces will manifests itself as a shift in the interaction, while the effect on the lipid head group will change the decay length and the range of the interaction.

The understanding of these subtle effects provides a powerful framework to study the interaction of a large number of solute molecules such as ions or small molecules such as peptides interacting directly or indirectly with the surface of lipid bilayers.

In light of this review of the literature on the measurements of the hydration interaction we can highlight a few similarities and differences when comparing the force laws obtained with solid and soft (fluid) surfaces. In terms of similarities, for both systems, the hydration force exhibits a monotonically decaying component whose decay length varies between 0.1 and 1 nm. The origin of this component is quite different in both systems: for solid surfaces it involves water molecules bound to the surfaces either directly or via strongly adsorbed ions, while for soft lipid bilayers it is related to the lipid head-group conformation and level of hydration. A clear evidence that origin of the hydration force in both systems is different can be appreciated in the fact that the hydration force between solid surfaces appears only above a critical salt concentration which is not the case for soft bilayers.

Hard atomically flat surfaces are the only system exhibiting an oscillatory component of the hydration superimposed to the monotically decaying component. The appearance of this component is in part related to water conformational polarization induced by the presence of ions on the surface.

403   Finally, it is important to remind that the appearance of the hydration force has been quite often
404   associated mainly to the ordering water molecules on the surfaces. Hydration forces rise from the
405   overlapping and therefore rearrangement of this ordering of water molecules. There is obviously
406   a connection between ordering/structuring of water and the hydration force, but both phenomena
407   should be always carefully distinguished.
408
409
410

References

411
412
413 [1] Derjaguin BV, Landau L. Acta Phys Chim URSS 1941;14.
314 [2] Verwey EJW, Overbeek JTG. Theory of stability of lyophobic colloids. Elsevier Amsterdam.
415 1948.
416 [3] Israelachvili JN. Measurement of hydration forces between macroscopic surfaces. Chem Scr.
417 1985;25:7-14.
418 [4] Frens G, Overbeek JTG. J Colloid Interface Sci. 1972;38.
419 [5] Overbeek JTG. J Colloid Interface Sci. 1977;58.
420 [6] Leneveu DM, Rand RP, Parsegian VA. Nature. 1976;259:601.
421 [7] Parsegian VA, Fuller N, Rand RP. Proc Natl Acad Sci USA. 1979;76:2750.
422 [8] Lis LJ, McAlsiter M, Fuller N, Rand RP, Parsegain VA. Biophys J. 1982;37:657.
423 [9] van Olpen H. An introduction to clay colloidal chemistry. Wiley: New York; 1977.
424 [10] Viani BE, Low PF, Roth CBJ. J Colloid Interface Sci. 1983;96:229.
425 [11] Rau DR, Lee BK, Parsegain VA. Proc Natl Acad Sci USA. 1984;81:2621.
426 [12] Tabor D, Winterton RHS. Proc R Soc Lond Ser A. 1969;312:435.
427 [13] Israelachvili JN, Tabor D. Proc R Soc Lond Ser A. 1972;331:19.
428 [14] Israelachvili JN, Tabor D. Prog Surf Membrane Sci. 1973;7:1.
429 [15] Huang J, Yan B, Faghihnejad A, Xu H, Zeng H. Understanding nanorheology and surface
430 forces of confined thin films. Korea-Australia Rheology Journal. 2014;26:3-14.
431 [16] Banquy X, Lee DW, Das S, Hogan J, Israelachvili JN. Shear-Induced Aggregation of
432 Mammalian Synovial Fluid Components under Boundary Lubrication Conditions. Advanced
433 Functional Materials. 2014;24:3152-61.
434 [17] Baimpos T, Shrestha BR, Hu Q, Genchev G, Valtiner M. Real-time multiple beam
435 interferometry reveals complex deformations of metal–organic-framework crystals upon
436 humidity adsorption/desorption. J Phys Chem C. 2015;119:16769-76.
437 [18] Shrestha BR, Baimpos T, Raman S, Valtiner M. Angstrom-resolved real-time dissection of
438 electrochemically active noble metal interface. ACS Nano. 2014;8.
439 [19] Shrestha BR, Hu Q, Baimpos T, Kristiansen K, Israelachvili JN, Valtiner M. Real-time
440 monitoring of aluminum crevice corrosion and its inhibition by vanadates with multiple beam
441 interferometry in a surface forces apparatus. J Electrochem Soc. 2015;162:C327-C32.
442 [20] Heo J, Kang T, Jang SG, Hwang DS, Spruell JM, Killops KL, et al. Improved Performance
443 of Protected Catecholic Polysiloxanes for Bioinspired Wet Adhesion to Surface Oxides. J Am
444 Chem Soc. 2012;134:20139-45.
445 [21] Israelachvili JN, McGuiggan PM. Forces between surfaces in liquids. Proc R Soc Lond Ser
446 A. 1988;241:795-800.
447 [22] Israelachvili JN, Min Y, Akbulut M, Alig A, Carver G, Greene W, et al. Recent advances in
448 the surface forces apparatus (SFA) technique. Rep Prog Phys. 2010;73:036601.
449 [23] Kang T, Amir RJ, Khan A, Ohshimizu K, Hunt JN, Sivanandan K, et al. Facile access to
450 internally functionalized dendrimers through efficient and orthogonal click reactions. Chem
451 Comm. 2010;46:1556-8.
452 [24] Raman S, Utzig T, Baimpos T, Shrestha BR, Valtiner M. Deciphering the scaling of single-
453 molecule interactions using Jarzynski's equality. Nature Communications. 2014;5.
454 [25] Israelachvili JN, Adams GE. Direct measurement of long range forces between two mica
455 surfaces in aqueous KNO_3 solution. Nature. 1976;262.

456 [26] Pashley RM. DLVO and hydration forces between mica surfaces in Li^+, Na^+, K^+, and Cs^+
457 electrolyte solutions: A correlation of double-layer and hydration forces with surface cation
458 exchange properties J Colloid Interface Sci. 1981;83:531-46.
459 [27] Pashley RM. Hydration forces between mica surfaces in aqueous electrolyte solutions. J
460 Colloid Interface Sci. 1981;80:153-62.
461 [28] Pashley RM, Israelachvili JN. Molecular layering of water in thin-films between mica
462 surfaces and its relation to hydration forces. J Colloid Interface Sci. 1984;101:511-23.
463 [29] Pashley RM. Hydration forces between mica surfaces in electrolyte solutions. J Colloid
464 Interface Sci. 1982;16:57-62.
465 [30] Hribar B, Southall NT, Vlachy V, Dill KA. How ions affect the structure of water. J Am
466 Chem Soc. 2002;124:12302-11.
467 [31] Goldberg R, Chai L, Perkin S, Kampf N, Klein J. Breakdown of hydration repulsion
468 between charged surfaces in aqueous Cs^+ solutions. Phys Chem Chem Phys. 2008;10:4939-45.
469 [32] Pashley RM, Israelachvili JN. DLVO and hydration forces between mica surfaces in Mg^{2+},
470 Ca^{2+}, Sr^{2+}, and Ba^{2+} chloride solutions. J Colloid Interface Sci. 1984;97:446-55.
471 [33] Israelachvili JN, Adams GE. Measurement of forces between two mica surfaces in aqueous
472 electrolyte solution in the range 0-100 nm. J Chem Soc, Faraday Trans 1. 1978;74:975-1001.
473 [34] Rabinovich YI, Derjaguin BV, Churaev NV. Direct measurements of long-range surface
474 forces in gas and liquid media. J Colloid Interface Sci. 1982;16:63-78.
475 [35] Ruckenstein E, Schiby D. On the origin of repulsive hydration forces between two mica
476 plates. Chem Phys Letters. 1983;95.
477 [36] Abraham FF. The interfacial density profile of a Lennard–Jones fluid in contact with a (100)
478 Lennard–Jones wall and its relationship to idealized fluid-wall systems: a Monte-Carlo
479 simulation. J Chem Phys 1978;68 3713-6.
480 [37] Rao M, Berne BJ, Percus JK, Kalos MH. J Chem Phys. 1979;71:3802.
481 [38] Israelachvili JN, Pashley RM. Molecular layering of water at surfaces and origin of
482 repulsive hydration forces. Nature. 1983;306:249-50.
483 [39] Ricci M, Spijker P, Voitchovsky K. Water-induced correlation between single ions imaged
484 at the solid-liquid interface. Nat Commun. 2014;5.
485 [40] Leng Y. Hydration force between mica surfaces in aqueous KCl electrolyte solution.
486 Langmuir. 2012;28:5339-49.
487 [41] Urbic T, Vlachy V, Dill KA. Confined water: A Mercedes-Benz model study. J Phys Chem
488 B. 2006;110:4963-70.
489 [42] Cherepanov DA. Force oscillations and dielectric overscreening of interfacial water. Phys
490 Rev Lett. 2004;93.
491 [43] Henderson D, Lozadacassou M. A simple theory for the force between spheres immersed in
492 a fluid. J Colloid Interface Sci. 1986;114:180-3.
493 [44] Li T-D, Gao J, Szoszkiewicz R, Landman U, Riedo E. Structured and viscous water in
494 subnanometer gaps. Phys Rev B. 2007;75.
495 [45] Fenter P, Lee SS. Hydration layer structure at solid-water interfaces. MRS Bull.
496 2014;39:1056-61.
497 [46] Cheng L, Fenter P, Nagy KL, Schlegel ML, Sturchio NC. Molecular-scale density
498 oscillations in water adjacent to a mica surface. Phys Rev Lett. 2001;87.
499 [47] Horn RG, Smith DT, Haller W. Surface forces and viscosity of water measured between
500 silica sheets. Chem Phys Lett. 1989;162:404-8.

[48] Vigil G, Xu ZH, Steinberg S, Israelachvili J. Interactions of silica surfaces. Journal of Colloid and Interface Science. 1994;165:367-85.

[49] Drucker WA, Senden TJ, Pashley RM. Measurement of forces in liquids using a force microscope Langmuir. 1992;8:1831-6

[50] Shubin VE, Kekicheff P. Electrical double-layer structure revisited via a surface force apparatus - mica interfaces in lithium-nitrate solutions. J Colloid Interface Sci. 1993;155:108-23.

[51] Ducker WA, Xu Z, Clarke DR, Israelachvili JN. Forces between alumina surfaces in salt-solutions - non-DLVO forces and the implications for colloidal processing. J Am Ceram Soc. 1994;77:437-43.

[52] Israelachvili JN. Intermolecular and surface forces. Third ed: Elsevier; 2011.

[53] Iler RK. The chemistry of silica. New York: Wiley; 1979.

[54] Claesson P, Horn RG, Pashley RM. Measurement of surface forces between mica sheets immersed in aqueous quaternary ammonium ion solutions. J Colloid Interface Sci. 1984;100:250-63.

[55] Ducker WA, Pashley RM. The forces between mica surfaces in ammonium-chloride solutions. J Colloid Interface Sci. 1989;131:433-9.

[56] Chapel JP. Electrolyte species dependent hydration forces between silica surfaces. Langmuir. 1994;10 4237–43.

[57] Drucker WA, Senden TJ, Pashley RM. Direct measurement of colloidal forces using atomic force microscope. Nature. 1991;353.

[58] Fielden ML, Hayes RA, Ralston J. Oscillatory and ion-correlation forces observed in direct force measurements between silica surfaces in concentrated $CaCl_2$ solutions. Phys Chem Chem Phys. 2000;2:2623-8.

[59] Vakarelski IU, Ishimura K, Higashitani K. Adhesion between silica particle and mica surfaces in water and electrolyte solutions. Journal of Colloid and Interface Science. 2000;227:111-8.

[60] Antognozzi M, Humphris ADL, Miles MJ. Observation of molecular layering in a confined water film and study of the layers viscoelastic properties. Appl Phys Lett. 2001;78:300-2.

[61] Jeffery S, Hoffmann PM, Pethica JB, Ramanujan C, Ozer HO, Oral A. Direct measurement of molecular stiffness and damping in confined water layers. Phys Rev B. 2004;70.

[62] Acuna SM, Toledo PG. Short-range forces between glass surfaces in aqueous solutions. Langmuir. 2008;24:4881-7.

[63] Tulpar A, Van Tassel PR, Walz JY. Structuring of macroions confined between like-charged surfaces. Langmuir. 2006;22:2876-83.

[64] Acuna SM, Toledo PG. Nanoscale repulsive forces between mica and silica surfaces in aqueous solutions. J Colloid Interface Sci. 2011;361:397-9.

[65] Loh S-H, Jarvis SP. Visualization of ion distribution at the mica-electrolyte interface. Langmuir. 2010;26:9176-8.

[66] Kilpatrick JI, Loh S-H, Jarvis SP. Directly Probing the Effects of Ions on Hydration Forces at Interfaces. J Am Chem Soc. 2013;135:2628-34.

[67] Ducker WA, Senden TJ, Pashley RM. Measurement Of Forces In Liquids Using A Force Microscope. Langmuir. 1992;8:1831-6.

[68] Atkins DT, Ninham BW. Surface and structural forces measured between silica surfaces in 1,2-ethanediol. Colloids Surf, A. 1997;129:23-32.

545 [69] Zeng Y, von Klitzing. R. Oscillatory forces of nanoparticle suspensions confined between
546 rough surfaces modified with polyelectrolytes via the layer-by-layer technique. Langmuir.
547 2012;28:6313-21.
548 [70] Yang K, Lin Y, Lu X, Neimark AV. Solvation forces between molecularly rough surfaces. J
549 Colloid Interface Sci. 2011;362:382-8.
550 [71] Akrami SMR, Nakayachi H, Watanabe-Nakayama T, Asakawa H, Fukuma T. Significant
551 improvements in stability and reproducibility of atomic-scale atomic force microscopy in liquid.
552 Nanotechnology. 2014;25.
553 [72] Liang Y, Hilal N, Langston P, Starov V. Interaction forces between colloidal particles in
554 liquid: Theory and experiment. Adv Colloid Interface Sci. 2007;134-35:151-66.
555 [73] Valle-Delgado JJ, Molina-Bolivar JA, Galisteo-Gonzalez F, Galvez-Ruiz MJ, Feiler A,
556 Rutland MW. Hydration forces between silica surfaces: Experimental data and predictions from
557 different theories. Journal of Chemical Physics. 2005;123:12.
558 [74] Butt HJ. Measuring electrostatic, vanderwaals, and hydration forces in electrolyte-solutions
559 with an atomic force microscope. Biophys J. 1991;60:1438-44.
560 [75] Meagher L. Direct measurement of forces between silica surfaces in aqueous $CaCl_2$
561 solutions using an atomic force microscope. J Colloid Interface Sci. 1992;152:293-5.
562 [76] Biggs S, Mulvaney P, Zukoski CF, Grieser F. Study of anion adsorption at the gold-aqueous
563 solution interface by atomic-force microscopy. J Am Chem Soc. 1994;116:9150-7.
564 [77] Karaman ME, Pashley RM, Waite TD, Hatch SJ, Bustamante H. A comparison of the
565 interaction forces between model alumina surfaces and their colloidal properties. Colloids and
566 Surf, A. 1997;129:239-55.
567 [78] Spaepen F. Structural model for the solid–liquid interface in monoatomic systems. Acta
568 Mettallurgica. 1975;23:729-43.
569 [79] Curtin WA. Density-functional theory of the solid-liquid interface. Phys Rev Lett.
570 1987;59:1228-31.
571 [80] Richens DT. The Chemistry of Aqua-Ions: John Wiley & Sons, Chichester; 1997.
572 [81] Spohr E. Computer-simulation of the water platinum interface. J Phys Chem. 1989;93:6171-
573 80.
574 [82] Spohr E. Computer-simulation of the water platinum interface - dynamic results. J Chem
575 Phys. 1990;141:87-94.
576 [83] Delville A. Structure and properties of confined liquids - A molecular-model of the clay
577 water interface. J Phys Chem. 1993;97:9703-12.
578 [84] Delville A, Sokolowski S. Adsorption of vapor at a solid interface - A molecular-model of
579 clay wetting. J Phys Chem. 1993;97:6261-71.
580 [85] Lee SH, Rossky PJ. A comparison of the structure and dynamics of liquid water at
581 hydrophobic and hydrophilic surfaces - a molecular-dynamics simulation study. J Chem Phys.
582 1994;100:3334-45.
583 [86] Vossen M, Forstmann F. The structure of water at a planar wall - an integral-equation
584 approach with the central force model. Journal of Chemical Physics. 1994;101:2379-90.
585 [87] Xia XF, Perera L, Essmann U, Berkowitz ML. The structure of water at platinum/water
586 interfaces - molecular-dynamics computer-simulations. Surf Sci. 1995;335:401-15.
587 [88] Bridgeman CH, Buckingham AD, Skipper NT, Payne MC. Ab-initio total energy study of
588 uncharged 2:1 clays and their interaction with water. Mol Phys. 1996;89:879-88.
589 [89] Bridgeman CH, Skipper NT. A Monte Carlo study of water at an uncharged clay surface. J
590 Phys Cond Mat. 1997;9:4081-7.

591 [90] Akiyama R, Hirata F. Theoretical study for water structure at highly ordered surface: Effect
592 of surface structure. J Chem Phys. 1998;108:4904-11.
593 [91] Yeh IC, Berkowitz ML. Structure and dynamics of water at water vertical bar Pt interface as
594 seen by molecular dynamics computer simulation. J Electroanal Chem. 1998;450:313-25.
595 [92] Stockelmann E, Hentschke R. A molecular-dynamics simulation study of water on
596 NaCl(100) using a polarizable water model. J Chem Phys. 1999;110:12097-107.
597 [93] Yeh IC, Berkowitz ML. Aqueous solution near charged Ag(111) surfaces: Comparison
598 between a computer simulation and experiment. Chemical Physics Letters. 1999;301:81-6.
599 [94] Wang J, Ocko BM, Davenport AJ, Isaacs HS. Insitu X-ray-diffraction and X-ray-reflectivity
600 studies of the Au(111) electrolyte interface—reconstruction and anion adsorption. Phys Rev B.
601 1992;46 10321–38.
602 [95] Toney MF, Howard JN, Richer J, Borges GL, Gordon JG, Melroy OR, et al. Voltage-
603 dependent ordering of water-molecules at an electrode-electrolyte interface. Nature.
604 1994;368:444-6.
605 [96] Toney MF, Howard JN, Richer J, Borges GL, Gordon JG, Melroy OR, et al. Distribution of
606 water-molecules at ag(111)/electrolyte interface as studied with surface X-ray-scattering. Surf
607 Sci. 1995;335:326-32.
608 [97] Chu YS, Lister TE, Cullen WG, You H, Nagy Z. Commensurate water monolayer at the
609 RuO2(110)/water interface. Phys Rev Lett. 2001;86:3364-7.
610 [98] Brown GE, Calas G, Waychunas GA, Petiau J. X-ray absorption-spectroscopy and its
611 applications in mineralogy and geochemistry. Rev Mineral. 1988;18:431-512.
612 [99] Brown GE, Parks GA. Synchrotron-based x-ray absorption studies of cation environments
613 in earth materials. Rev Geophys. 1989;27:519-33.
614 [100] Feidenhansl R. Surface-structure determination by x-ray-diffraction. Surf Sci Rep.
615 1989;10:105-88.
616 [101] Robinson IK, Tweet DJ. Surface X-ray-diffraction. Rep Prog Phys. 1992;55:599-651.
617 [102] Brown GE, Parks GA. Sorption of trace elements on mineral surfaces: Modern
618 perspectives from spectroscopic studies, and comments on sorption in the marine environment.
619 Int Geol Rev. 2001;43:963-1073.
620 [103] Bedzyk MJ, Cheng LW. X-ray standing wave studies of minerals and mineral surfaces:
621 Principles and applications. In: Fenter PA, Rivers ML, Sturchio NC, Sutton SR, editors.
622 Applications of Synchrotron Radiation in Low-Temperature Geochemistry and Environmental
623 Sciences2002. p. 221-66.
624 [104] Huisman WJ, Peters JF, Zwanenburg MJ, deVries SA, Derry TE, Abernathy D, et al.
625 Layering of a liquid metal in contact with a hard wall. Nature. 1997;390:379-81.
626 [105] Yu CJ, Richter AG, Kmetko J, Datta A, Dutta P. X-ray diffraction evidence of ordering in
627 a normal liquid near the solid–liquid interface. Europhys Lett. 2000;50:487–93.
628 [106] Yu CJ, Richter AG, Datta A, Durbin MK, Dutta P. Observation of molecular layering in
629 thin liquid films using X-ray reflectivity. Phys Rev Lett. 1999;82:2326-9.
630 [107] Doerr AK, Tolan M, Schlomka JP, Press W. Evidence for density anomalies of liquids at
631 the solid/liquid interface. Europhys Lett. 2000;52:330-6.
632 [108] Yu CJ, Evmenenko G, Kmetko J, Dutta P. Effects of shear flow on interfacial ordering in
633 liquids: X-ray scattering studies. Langmuir. 2003;19:9558-61.
634 [109] Skipper NT, Soper AK, McConnell JDC. The structure of interlayer water in vermiculite. J
635 Chem Phys. 1991;94:5751-60.

636 [110] Karaborni S, Smit B, Heidug W, Urai J, vanOort E. The swelling of clays: Molecular
637 simulations of the hydration of montmorillonite. Science. 1996;271:1102-4.
638 [111] Sposito G, Skipper NT, Sutton R, Park SH, Soper AK, Greathouse JA. Surface
639 geochemistry of the clay minerals. Proc Natl Acad Sci U S A. 1999;96:3358-64.
640 [112] Skipper NT, Williams GD, de Siqueira AVC, Lobban C, Soper AK. Time-of-flight neutron
641 diffraction studies of clay-fluid interactions under basin conditions. Clay Miner. 2000;35:283-90.
642 [113] Geissbuhler P, Fenter P, DiMasi E, Srajer G, Sorensen LB, Sturchio NC. Three-
643 dimensional structure of the calcite-water interface by surface X-ray scattering. Surf Sci.
644 2004;573:191-203.
645 [114] Fenter P, Sturchio NC. Calcite (104)-water interface structure, revisited. Geochim
646 Cosmochim Acta. 2012;97:58-69.
647 [115] Zhou H, Ganesh P, Presser V, Wander MCF, Fenter P, Kent PRC, et al. Understanding
648 controls on interfacial wetting at epitaxial graphene: Experiment and theory. Phys Rev B.
649 2012;85.
650 [116] Lee SS, Fenter P, Nagy KL, Sturchio NC. Monovalent ion adsorption at the muscovite
651 (001)-solution interface: Relationships among ion coverage and speciation, interfacial water
652 structure, and substrate relaxation. Langmuir. 2012;28:8637-50.
653 [117] Lee SS, Fenter P, Nagy KL, Sturchio NC. Changes in adsorption free energy and
654 speciation during competitive adsorption between monovalent cations at the muscovite (001)-
655 water interface. Geochim Cosmochim Acta. 2013;123:416-26.
656 [118] Fenter P, Kerisit S, Raiteri P, Gale LD. Is the Calcite–Water Interface Understood? Direct
657 Comparisons of Molecular Dynamics Simulations with Specular X-ray Reflectivity Data. J Phys
658 Chem C. 2013;117:5028–42.
659 [119] Fenter P, Sturchio NC. Mineral-water interfacial structures revealed by synchrotron X-ray
660 scattering. Prog Surf Sci. 2004;77:171-258.
661 [120] Binder H. The molecular architecture of lipid membranes - New insights from hydration-
662 tuning infrared linear dichroism spectroscopy. Appl Spectrosc Rev. 2003;38:15-69.
663 [121] Aman K, Lindahl E, Edholm O, Hakansson P, Westlund PO. Structure and dynamics of
664 interfacial water in an L-alpha phase lipid bilayer from molecular dynamics simulations. Biophys
665 J. 2003;84:102-15.
666 [122] Marsh D. Handbook of lipid bilayers. 2nd ed. Boca Raton, FL.: CRC Press, Taylor &
667 Francis Group; 2013.
668 [123] Pandit SA, Bostick D, Berkowitz ML. Mixed bilayer containing
669 dipalmitoylphosphatidylcholine and dipalmitoylphosphatidylserine: Lipid complexation, ion
670 binding, and electrostatics. Biophys J. 2003;85:3120-31.
671 [124] Berkowitz ML, Bostick DL, Pandit S. Aqueous solutions next to phospholipid membrane
672 surfaces: insights from simulations. Chemical reviews. 2006;106:1527-39.
673 [125] Bockmann RA, Hac A, Heimburg T, Grubmuller H. Effect of sodium chloride on a lipid
674 bilayer. Biophys J. 2003;85:1647-55.
675 [126] Pandit SA, Bostick D, Berkowitz ML. Mixed bilayer containing
676 dipalmitoylphosphatidylcholine and dipalmitoylphosphatidylserine: lipid complexation, ion
677 binding, and electrostatics. Biophys J. 2003;85:3120-31.
678 [127] Schrader AM, Donaldson SH, Jr., Song J, Cheng CY, Lee DW, Han S, et al. Correlating
679 steric hydration forces with water dynamics through surface force and diffusion NMR
680 measurements in a lipid-DMSO-H2O system. Proceedings of the National Academy of Sciences
681 of the United States of America. 2015;112:10708-13.

682 [128] Yu J, Wei W, Danner E, Israelachvili JN, Waite JH. Effects of Interfacial Redox in Mussel
683 Adhesive Protein Films on Mica. Adv Mater. 2011;23:2362-6.
684 [129] Rand RP, Fuller NL, Lis LJ. Myelin Swelling and Measurement of Forces between Myelin
685 Membranes. Nature. 1979;279:258-60.
686 [130] Degennes PG. Penetration of a Coil into an Adsorbed Layer - Application to the Kinetics
687 of Exchange and to Bridging Processes between Colloidal Particles. Cr Acad Sci Ii.
688 1985;301:1399-403.
689 [131] Degennes PG. Polymers at an Interface - a Simplified View. Adv Colloid Interfac.
690 1987;27:189-209.
691 [132] Harbich W, Servuss RM, Helfrich W. Passages in Lecithin-Water Systems. Z Naturforsch
692 A. 1978;33:1013-7.
693 [133] Donaldson SH, Lee CT, Chmelka BF, Israelachvili JN. General hydrophobic interaction
694 potential for surfactant/lipid bilayers from direct force measurements between light-modulated
695 bilayers. Proceedings of the National Academy of Sciences of the United States of America.
696 2011;108:15699-704.
697 [134] Donaldson SH, Royne A, Kristiansen K, Rapp MV, Das S, Gebbie MA, et al. Developing
698 a General Interaction Potential for Hydrophobic and Hydrophilic Interactions. Langmuir.
699 2015;31:2051-64.
700 [135] Sanchez-Iglesias A, Grzelczak M, Altantzis T, Goris B, Perez-Juste J, Bals S, et al.
701 Hydrophobic Interactions Modulate Self-Assembly of Nanoparticles. Acs Nano. 2012;6:11059-
702 65.
703 [136] Aniansson EAG, Wall SN, Almgren M, Hoffmann H, Kielmann I, Ulbricht W, et al.
704 Theory of Kinetics of Micellar Equilibria and Quantitative Interpretation of Chemical Relaxation
705 Studies of Micellar Solutions of Ionic Surfactants. J Phys Chem-Us. 1976;80:905-22.
706 [137] Aniansson GEA. Dynamics and Structure of Micelles and Other Amphiphile Structures. J
707 Phys Chem-Us. 1978;82:2805-8.
708 [138] Banquy X, Kristiansen K, Lee DW, Israelachvili JN. Adhesion and hemifusion of
709 cytoplasmic myelin lipid membranes are highly dependent on the lipid composition. Bba-
710 Biomembranes. 2012;1818:402-10.
711 [139] Donaldson S, Chmelka BF, Israelachvili JN. General hydrophobic interaction potential for
712 surfactant/lipid bilayers from direct force measurements between light-modulated bilayers Proc
713 Natl Acad Sci USA. 2011;108:15699-704.
714 [140] Mitchell DJ, Ninham BW. Curvature Elasticity of Charged Membranes. Langmuir.
715 1989;5:1121-3.
716 [141] Schrader AM, Donaldson SH, Song J, Cheng CY, Lee DW, Han S, et al. Correlating steric
717 hydration forces with water dynamics through surface force and diffusion NMR measurements in
718 a lipid-DMSO-H2O system. Proceedings of the National Academy of Sciences of the United
719 States of America. 2015;112:10708-13.
720 [142] Schneck E, Sedlmeier F, Netz RR. Hydration repulsion between biomembranes results
721 from an interplay of dehydration and depolarization. Proceedings of the National Academy of
722 Sciences of the United States of America. 2012;109:14405-9.
723 [143] Israelachvili JN, Wennerstrom H. Entropic Forces between Amphiphilic Surfaces in
724 Liquids. J Phys Chem-Us. 1992;96:520-31.
725 [144] Mcintosh TJ, Simon SA. Contributions of Hydration and Steric (Entropic) Pressures to the
726 Interactions between Phosphatidylcholine Bilayers - Experiments with the Subgel Phase.
727 Biochemistry-Us. 1993;32:8374-84.

728